Int. J. Electrochem. Sci., 10 **(2015)** 4532 - 4551

International Journal of
ELECTROCHEMICAL
SCIENCE
www.electrochemsci.org

Electrochemical Studies of 1-(2-(4-nitrophenyl)-2-oxoethyl)pyridazinium bromide, On Carbon Steel Corrosion in Hydrochloric Acid Medium

M. Messali[1,*], *A. Bousskri*[2], *A. Anejjar*[2], *R. Salghi*[2], *B. Hammouti*[3]

[1] Chemistry Department, Faculty of Science, Taibah University, 30002, Al-Madinah Al-Mounawwara, Saudi Arabia
[2] Laboratory of Environmental Engineering and Biotechnology, ENSA, Ibn Zohr University, Box 1136, 80000 Agadir, Morocco
[3] LCAE-URAC 18, Faculty of Science, University of Mohammed Premier, Box 717, 60000 Oujda, Morocco
[*]E-mail: mouslim@mail.be

Received: 16 March 2015 / *Accepted:* 16 April 2015 / *Published:* 28 April 2015

The corrosion performance of Carbon steel in HCl solution with different concentration of synthesized Pyridazinium-based Ionic liquids namely: 1-(2-(4-nitrophenyl)-2-oxoethyl)pyridazinium bromide NPEPB, was investigated by electrochemical measurements and weight loss. The obtained results reveal that NPEPB performs excellently as good corrosion inhibitor for Carbon steel in 1.0 M HCl. Polarization curves studies indicated that NPEPB behaves as mixed-type inhibitors. The calculated inhibition efficiencies from weight loss measurements, show the same evolution as those obtained from electrochemical studies. Also, the inhibition efficiency was found to increase with increase of the inhibitor concentrations to reach 85 % at 10^{-3}M of NPEPB due to the adsorption of the inhibitors molecule on the electrod surface. Impedance measurements spectra exhibit one capacitive and valid the inhibitive ability. confirming that this inhibitor inhibits the corrosion in 1 M HCl through adsorption process following Langmuir adsorption isotherm. Some thermodynamic functions of the carbon steel dissolution process in acid medium were also determined and discussed.

Keywords: Corrosion, Adsorption, C-Steel, Pyridazinium-based ionic liquid, Acid medium.

1. INTRODUCTION

Hydrochloric acid solutions are largely used in chemical and several industrial processes such as acid cleaning, acid descaling, acid oil well acidizing and pickling, Because of the aggressiveness of acid solutions, inhibitors are ordinarily used to reduce the corrosive attack on metallic electrod [1-5].

Organic compounds contain the heteroatoms such as nitrogen, sulphur and oxygen generally exhibit the best protection for the metal [6-36]. The inhibitor adsorption mode was dependent on the inhibitor structure [35]. Data in the literature show that most organic inhibitors adsorb on metals by displacing water molecules on the surface of electrode to forming a compact barrier film on the metal [35–37].The development of new corrosion inhibitors of non-toxic nature, which do not contain heavy metals and organic phosphates, is very important [38]. The inhibitors can decrease the dissolution rate of metals, affecting the kinetics of the reactions which create the corrosion process. Although Pyridazinium-based ionic liquids (ILs) are expected to be good candidates as corrosion inhibitors because of their environmentally friendly characteristics in addition to their unique properties [39-41], little investigations have been found in literature [42-43]. Zhang et al [44] have investigated the behavior of alkylimidazolium ionic liquids for steel in acidic medium. This confirmed that ILs revealed excellent inhibition performance for mild steel in acidic solution. Imidazolium compounds are reported to show corrosion resistant behavior of copper [45], steel [46] and aluminum [47]. It is found that the action of such inhibitors depends on the specific interaction between the functional groups and the metal surface, due to the presence of the –C=N- group and electronegative nitrogen in the molecule. In the present work, the objective was to study the inhibition effect of a pyridazinium-based ionic liquid (IL) compound, namely the 11-(2-(4-nitrophenyl)-2-oxoethyl)pyridazinium bromide (NPEPB), on the corrosion of carbon steel in 1M HCl. Electrochemical behavior experiments were done in HCl media in the presence and absence of inhibitor using the weight loss method, potentiodynamic polarization and electrochemical impedance spectroscopic (EIS) studies. The chemical structure of the studied Pyridazinium ionic liquid is given in Fig 1. It is also aimed to predict the adsorption behavior and to study his thermodynamic feasibility of adsorption of the IL inhibitor molecule on steel surface.

2. EXPERIMENTAL

2.1. Materials

The metal that we are used in this study is a carbon steel (C38) (Euronorm: C35E carbon steel and US specification: SAE 1035) with a chemical composition (in wt%) of 0.370 % C, 0.230 % Si, 0.680 % Mn, 0.077 % Cr, 0.016 % S, 0.011 % Ti, 0.009 % Co, 0.059 % Ni, 0.160 % Cu and the remainder iron (Fe).

2.2. Chemical structure of 1-(2-(4-nitrophenyl)-2-oxoethyl)pyridazinium bromide (NPEPB).

Microwave or ultrasound-assisted synthesis and characterization of various imidazolium, piridinium and pyridazinium-based ionic liquids (ILs) was reported in details by M.Messali *et al*. [49-53]. The structure of the investigated (IL) in the current work, namely, *1-(2-(4-nitrophenyl)-2-oxoethyl)pyridazinium bromide* is shown in Figure.1. In the following text, this compound will be denoted as NPEPB for simplicity.

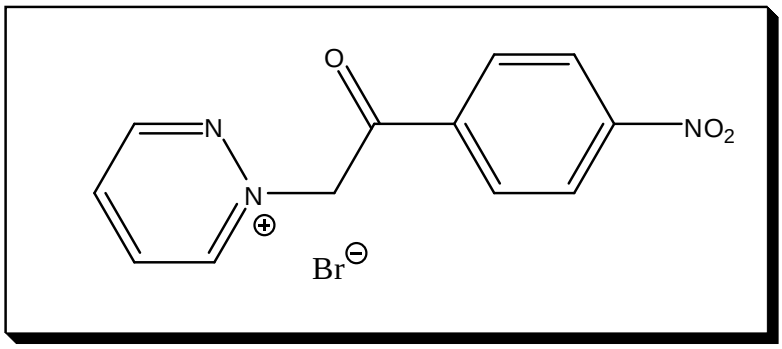

Figure 1. Structure of 1-(2-(4-nitrophenyl)-2-oxoethyl)pyridazinium bromide (NPOPB).

2.3. Synthesis of 1-(2-(4-nitrophenyl)-2-oxoethyl)pyridazinium bromide (NPEPB).under Ultrasonic irradiation

Pyridazine (1 eq) and 2-bromo-1-(4-nitrophenyl)ethanone (1eq) were placed in a closed container and exposed to irradiation for five hours at 70 ºC using a sonication bath. Completion of the reaction was marked by the precipitation of a solid from the initially obtained clear and homogenous mixture in toluene. The obtained product was isolated by filtration and washed three times with Ethyl acetate solution to remove any unreacted starting materials and solvent. Afterwards, the pyridazinium salt was washed with ethyl acetate. Finally the IL was dried at a reduced pressure to remove all volatile organic compounds.

Although 1-(2-(4-nitrophenyl)-2-oxoethyl)pyridazinium bromide (NPEPB) have been previously reported by conventional methods [48], its preparation under ultrasound irradiation has never been disclosed. 1-(2-(4-nitrophenyl)-2-oxoethyl)pyridazinium bromide (NPEPB) was characterized by ^{1}H NMR, ^{13}C NMR, IR, and LCMS. ^{1}H NMR (400 MHz) and ^{13}C NMR (100 MHz) spectra were measured in DMSO at room temperature. Chemical shifts (δ) were reported in ppm calibrated to tetramethylsilane (TMS) as an internal standard. LCMS spectra were measured with a Micromass LCT mass spectrometer. IR spectra were recorded in an NaCl disc on a Shimadzu 8201 PC FTIR spectrophotometer (ν_{max} in cm^{-1}). The ultrasound-assisted reactions were performed using a high intensity ultrasonic processor SUB Aqua 5 Plus-Grant with temperature controller (750 W), microprocessor control, and 25 kHz ultrasonic frequency.

2.4. Characterization of 1-(2-(4-nitrophenyl)-2-oxoethyl)pyridazinium bromide (NPEPB).

Brown crystals, yield 80%, ^{1}H NMR (400MHz, DMSO) δ: 6.87 (s, 2H), 7.75 (dd, 2H), 8.13 (dd, 2H), 8.82 (dd, 1H), 8.94 (dd, 1H), 9.78 (dd, 1H), 10.05 (dd, 1H); ^{13}C NMR (100MHz, DMSO) δ: 189.7 (CO), 154.7 (CH), 151.8 (CH), 150.7 (C), 137.9 (C), 137.6 (CH), 136.0 (CH), 129.9, 124.1 (CH), 70.5 (CH_2); IR (νmax cm^{-1}) 3132 (C-H, sp 2), 1637 (C=O), 1597-1469 (C=C), 1165(C-N); LCMS (M-Br) 244.2 found for $C_{12}H_{10}N_3O_3^+$.

2.5. Solutions

The aggressive solutions of 1.0 M HCl were prepared by dilution of analytical grade 37% HCl with distilled water. The solution tests are freshly prepared before each experiment. The organic compound tested was the ionic liquid 1-(2-(4-nitrophenyl)-2-oxoethyl)pyridazinium bromide (NPEPB). The concentration range of the study of this compound was 10^{-3} to 10^{-6} M. Triplicate experiences were made to ensure the reproducibility.

2.6. Weight loss measurements

Specimens were cut into 2 × 2 × 0.08 cm^3 dimensions are used for the weight loss measurements method. Before all measurements, the exposed area was mechanically abraded with 180, 320, 800, 1200 grades of emery papers. The coupons were washed completely with bidistilled water then with acetone to provide the removal of all corrosion products, and finally degreased and dried with ethanol solution before weighing. Weight loss measurements are performed in a double walled glass cell equipped with a thermostated cooling condenser. The solution volume that we used for each measurement is 80 cm^3. The immersion time for the weight loss is 6 h at temperatur 298 K. All experiments were duplicated to guarantee reproducibility and the mean values are reported in the current work.

2.7. Electrochemical tests

2.7.1. Electrochemical Impedance Spectroscopy

Impedance measurements are performed at 298K after 1/2 hours of immersion in acid medium by using Voltalab (Tacussel-Radiometer PGZ 100) potentiostat and piloted by Voltamaster software under static condition. Electrochemical measurements were performed in a three electrode cylindrical glass cell. The platinum electrode and a saturated calomel electrode (SCE) were used as auxiliary and reference electrodes, respectively. All potentials given in this study were referred to SCE reference electrode. The working electrode used in this study was the same used for gravimetric measurements. The working electrode was immersed in test solution for 30 minutes to establish asteady state open circuit potential (Eocp). After measuring the Eocp, the electrochemical measurements were carried out. All electrochemical tests have been performed in aerated solutions at 298 K. The EIS experiments were conducted in the frequency range with high limit of 100 kHz and different low limit 0.1 Hz at open circuit potential, with 10 points per decade, at the rest potential, after 30 min of acid immersion, by applying 10 mV ac voltage peak-to-peak. Nyquist plots were made from these experiments and the impedence plots are given in the Nyquist representation. Experiments are repeated three times to ensure the reproducibility.

2.7.2. Potentiodynamic polarization

In this study the electrochemical behaviour of carbon steel electrod in inhibited and uninhibited solution was studied by chek in anodic and cathodic potentiodynamic polarization curves. Measurements were carried out in the 1.0 M of chloridric acid solution containing different concentrations of the studied inhibitor by changing the electrode potential from -800 mV to -200 mV versus corrosion potential at a scan rate of 1 $mV.s^{-1}$. The linear Tafel segments of anodic and cathodic curves were extrapolated to corrosion potential to obtain corrosion current densities (I_{corr}).

2.8. Optical microscopy

Immersion corrosion analysis of carbon steel specimen in the acidic solutions with and without inhibitor was carried out using Optical microscopy (OM). After the corrosion tests, the samples were submitted to OM studies to know the surface morphology. OM ***Est Scope*** was used for the experiments.

3. RESULTS AND DISCUSSION

3.1 Potentiodynamic Polarization Curves

Fig.2 show the anodic and cathodic polarization curves for carbon steel in 1M HCl at different concentrations of the NPEPB inhibitor

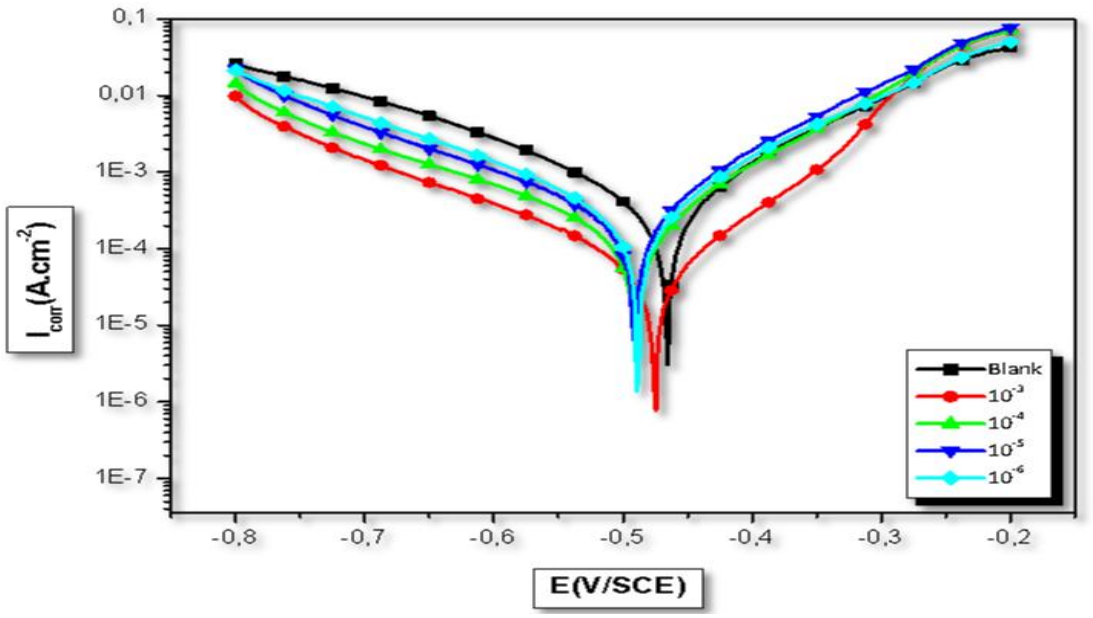

Figure 2. Potentiodynamic polarization curves of C38 steel in 1M HCl in the presence of different concentrations of NPEPB at 298 K.

It's clear from this figure that the addition of the inhibitor concentration causes a significant decrease in the corrosion rate, a displacement of the anodic curves to more positive potentials and the cathodic curves to more negative potentials. This may be attributed to adsorption of the inhibitor on the electrod surface. Fig. 2 shows the Tafel polarization curves for C-steel in 1.0 M chloridric acid solution at different concentrations (10^{-3} to 10^{-6} M) of inhibitor at 298 K. The inhibition efficiency values E_I(%), were calculated using the following equation (1).

$$E_I\ \% = \frac{I_{corr} - I'_{corr}}{I_{corr}} \times 100 \quad (1)$$

Where I_{corr} and I'_{corr} are uninhibited and inhibited corrosion current densities, respectively. Values of the corrosion current densities (I_{corr}), corrosion potential (E_{corr}), cathodic Tafel slope (bc), were calculated from Figure1 and are listed in Table1.

Table 1. Electrochemical parameters of carbon steel in 1M HCl solution without and with NPEPB at different concentrations.

Inhibitor	Conc (M)	- E_{corr} (mV/SCE)	I_{corr} (µA/cm^2)	- b_c (mV/dec)	E_I (%)
BlanK	1.0	469	588	168	-
NPEPB	1×10^{-3}	478	78	168	**87**
	1×10^{-4}	493	183	174	69
	1×10^{-5}	493	256	168	54
	1×10^{-6}	491	325	168	44

Data in Table 1 show that NPEPB inhibits the corrosion process and the inhibition efficiency values E_I (%) increases with C_{inh}, reaching its maximum value 87%, at 10^{-3}M, due to the increase in the protect film of the electrode surface by adsorption. The values of the cathodic Tafel lines b*c*, show slight changes with the addition of NPEPB. This result means that the mechanism at the electrode reactions is not changed [54]. These data show that the increase in inhibitor concentration leads to decrease in the corrosion current density. The presence of the NPEPB concentration does not remarkable displacement of the corrosion potential, while the cathodic Tafels slopes bc change with the increase in the inhibitor concentration. These observations indicate that the NPEPB inhibitor is a mixed-type inhibitor for the corrosion of C-steel in 1.0 M HCl[55]. This due to the adsorption of the inhibitor on the corroding surface [56, 57].

3.2 Electrochemical Impedance Spectroscopy measurements

The impedance measurements were carried out at room temperature after 30 min of immersion in 1M HCl solutions in the absence and presence of different concentrations of the inhibitor NPEPB inhibitor. The Nyquist plots for carbon steel obtained at the interface in the presence and the absence of NPEPB at different concentrations are given in Fig. 3.

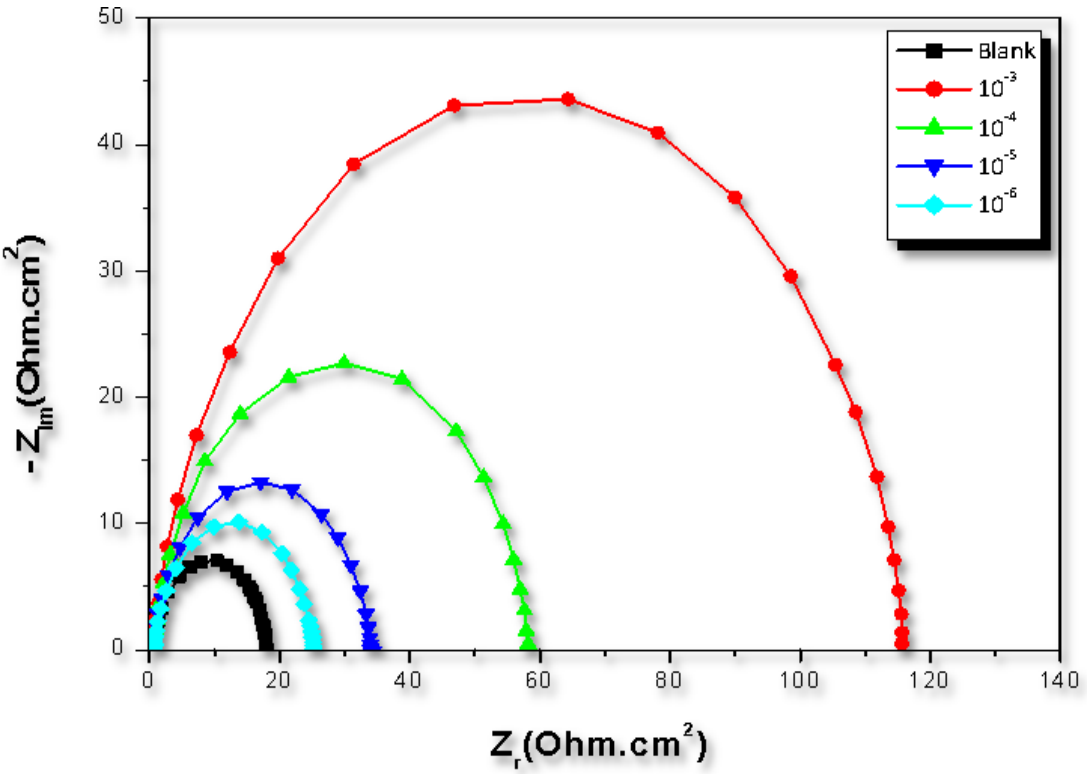

Figure 3. Nyquist plots for carbon steel in 1 M HCl containing different concentrations of NPEPB.

The charge-transfer resistance (R_{ct}) values are calculated from the difference in impedance at lower and higher frequencies as suggested by Tsuru et al [58]. The double layer capacitance (C_{dl}) and the frequency at which the imaginary component of the impedance is maximal ($-Z_{max}$) are found as represented in equation 2:

$$C_{dl} = \frac{1}{\omega R_{ct}} \quad \text{where} \quad \omega = 2\pi f_{max} \qquad (2)$$

Fig 3 show the Nyquist plots present capacitive loops as a depressed semicircle, the diameter of the capacitive loop in the presence of inhibitor is larger than that in the absence of inhibitor and increases with the inhibitor concentration, indicating that the corrosion is primarily a charge transfer process and the formed inhibitive film increases by the addition of the inhibitor NPEPB [59]. The impedance data were present in Table 2.

Table 2. Electrochemical Impedance for corrosion of steel in acid medium at various concentrations of NPEPB.

Inhibitor	Conc (M)	R_{ct} ($\Omega.cm^2$)	C_{dl} ($\mu F/cm^2$)	E_{Rct} (%)
BlanK	1	18	177	-
NPEPB	**1×10^{-3}**	117	55	**85**
	1×10^{-4}	58	69	69
	1×10^{-5}	34	74	47
	1×10^{-6}	25	101	28

The percent inhibition efficiency is calculated by charge transfer resistance obtained from Nyquist plots as follow [60].:

$$E_{Rct}\ \% = \frac{R'_{ct} - R_{ct}}{R'_{ct}} \times 100 \qquad (3)$$

Where R_{ct} and R'_{ct} are the charge transfer resistance values in absence and the presence ofinhibitor, respectively.

It is clear that, the corrosion of carbon steel in 1M HCl is clearly inhibited in the presence of the inhibitor, and the impedance response change with the increase in inhibitor concentration. Equivalent circuit as depicted in Fig.4 describes the metal / electrolyte interface of the present corroding system was used to simulate the impedance data in Fig.3.

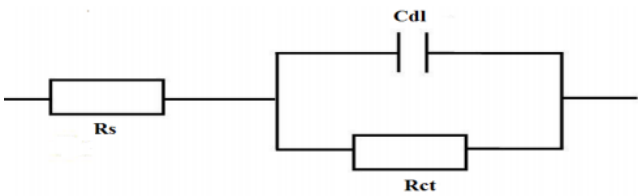

Figure 4. The standard Randle circuit.

From the Table 2, the maximum percentage of inhibition efficiency (E_{Rct} %) was achieved at the concentration of 10^{-3}M (85%). In the presence of the NPEPB the values of R_{ct} has enhanced and the values of double layer capacitance C_{dl} are also brought down to the maximum extent with the increasing of the inhibitors concentration. The decrease in C_{dl} shows that the adsorption of the inhibitors takes place on the metal surface in acidic solution; which can result from a decrease in local dielectric constant and/or an increase in the thickness of the electric double layer [61].The quantitative analysis of the electrochemical impedance spectra (EIS) was studied based on a physical model of the corrosion process with hydrogen depolarization and with charge transfer controlling step. The simplest model includes the charge transfer resistance (R_{ct}) in parallel to the capacitance (C_{dl}) connected with the solution resistance (R_s).

3.3. Weight Loss Measurements and adsorption isotherm

The effect of addition of NPEPB compound tested at different concentrations on the corrosion of steel in in 1.0 M HCl solution was studied by weight loss at 298K after 6h of immersion.

The values of the percentage inhibition efficiency E_W(%) were calculated from the following equation:

$$E_w\ \% = \frac{W_{corr} - W'_{corr}}{W_{corr}} \times 100 \qquad (5)$$

where W_{corr} and W'_{corr} are weight loss in the absence and presence of inhibitor. The rate of corrosion ρ (mg. cm^{-2}. h^{-1}) was calculated from equation:

$$\rho = \frac{w^{\circ} - w}{St} \quad (6)$$

where S is surface area of stadied steel plate and t is immersion time.

Table 3. Weight loss data of carbon steel in 1 M HCl for various concentration of the NPEPB.

Inhibitor	Conc. (M)	ρ (mg. cm^{-2} . h^{-1})	E_w (%)	Θ
BlanK	1	1.001	-	-
NPEPB	1×10^{-3}	0.1412	**85.89**	0.858
	1×10^{-4}	0.2901	71.02	0.710
	1×10^{-5}	0.4502	55.02	0.550
	1×10^{-6}	0.5924	40.82	0.408

The adsorption process depends on the structural formula and electronic characteristics of the inhibitor, steric effects, temperature, the nature of metal surface and the varying degrees of surface-site activity [62, 63]. In actual fact, the H_2O molecules could be adsorbed at the electrod/solution interface. To this effect, the adsorption of organic inhibitor molecules can be considered as a quasi substitution process between the organic compounds in the aqueous phase $Org_{(sol)}$ and water molecules at the electrode surface $H_2O_{(ads)}$ [64]:

$$Org_{(sol)} + xH_2O_{(ads)} \leftrightarrow xH_2O_{(sol)} + Org_{(ads)} \quad (4)$$

Where ***x*** is the size ratio that is the number of water molecules replaced by one organic inhibitor.

As can be seen from Table 3, that inhibitor NPEPB inhibits the corrosion of carbon steel and the efficiency inhibition increases with the increasing inhibitor concentration. This is better visualized in Fig.5 that shows the significant decrease in the corrosion rate (ρ) upon addition of NPEPB to the aggressive corrosion solution to reach a minimum value when as less as 10^{-6} M of NPEPB concentration is attained. This tremendous change in the corrosion rate values had a very strong impact on the inhibition efficiency, which in its turn increases with increasing NPEPB concentrations as depicted from table 4 and plotted in Fig. 5 reaching the highest value of E_w. 85.89 % at an NPEPB concentration of 10^{-3} M. These weight loss method are in good accord with the results of polarization curves corrosion tests and impedance measurements.

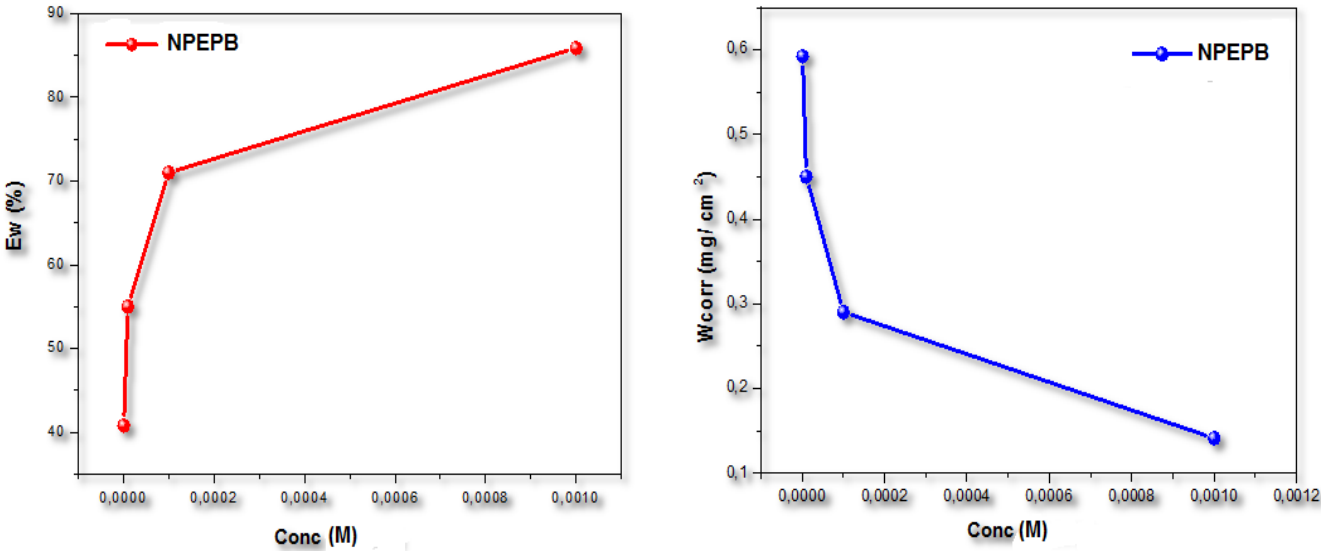

Figure 5. Variation of the inhibition efficiency (E_w %) and corrosion rate (W_{corr}) of carbon steel corrosion with the concentration of NPEPB in 1M HCl at 298 K.

The adsorption isotherm helps us to provid the information on the interaction between the inhibitor molecule of NPEPB and the metal surface. The degree of surface coverage (θ) for different concentrations of inhibitor was evaluated from Weight loss measurements. Attempts were made to fit θ values to various isotherms such as Temkin, Frumkin and Langmiur. The best fit was obtained with the Langmiur isotherm (Fig. 6). From this isotherm θ is linked to concentration inhibitor follow equation 7 [65].

$$\frac{\theta}{1-\theta} = K_{ads}.C_{inh} \qquad (7)$$

By rearranging this equation:

$$\frac{C_{inh}}{\theta} = \frac{1}{K_{ads}} + C_{inh} \qquad (8)$$

Where K_{ads} is the adsorption/desorption equilibrium constant, C_{inh} is the corrosion inhibitor concentration in the solution

$$\log K_{ads} = -1{,}74 - \left(-\frac{\Delta G^0_{ads}}{2.303RT} \right) \qquad (9)$$

Where ΔG^0_{ads} is the free energy of adsorption

It was found that from Fig.6 (plot of $\frac{C}{\theta}$ versus C) gives straight line with slope near to 1, indicating that the adsorption of compound under consideration on Carbon steel / acidic solution interface obeys Langmiur's adsorption. The thermodynamic parameters for the corrosion of carbon steel in 1 M of chloridric acid in the presence and absence of different concentrations of NPEPB is given in the Table 4.

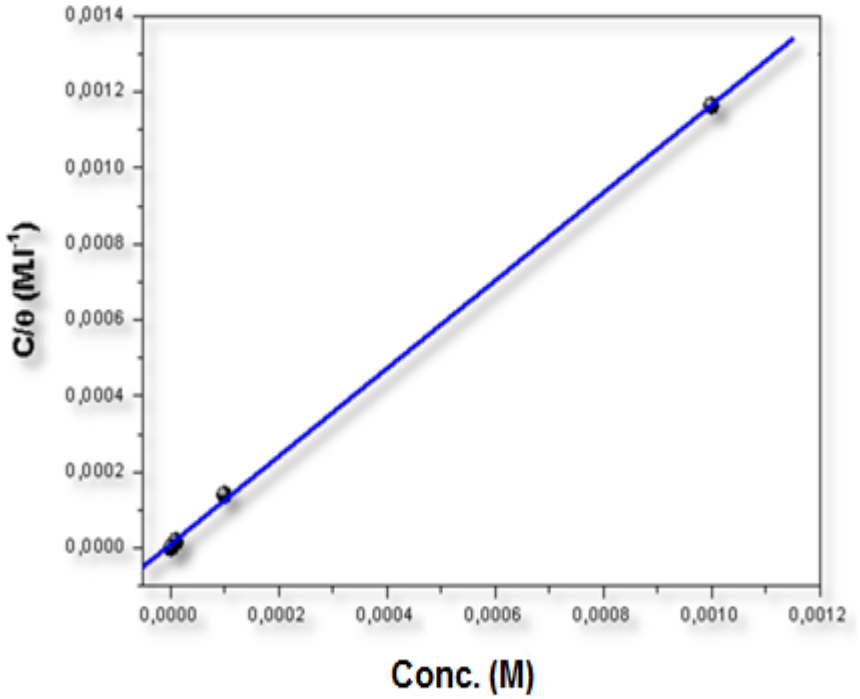

Figure 6. Plots of Langmuir adsorption isotherm of NPEPB on the steel surface at 298K.

Table 4. The thermodynamic parameters for the corrosion of carbon steel in 1 M HCl in the absence and presence of different concentrations of NPEPB.

Inhibitor	Slope	K_{ads} (M^{-1})	R^2	ΔG^0_{ads} (kJ/mol)
NPEPB	1.155	$9.43x10^4$	0.99	**- 38.31**

The free energy of adsorption ΔG^0_{ads} can be calculated from the K_{ads} value obtained from the above correlation [66]:

$$\Delta G_{ads} = -RT \ln \quad (55.5 \text{ x } K_{ads}) \qquad (10)$$

where 55.5 is the concentration of water, R (8.314J.K^{-1}.mol^{-1}) is the universal gas constant and T is the absolute temperature(K), K_{ads} the adsorption–desorption equilibrium constant.

The ΔG^0_{ads} values are also presented in Table 4, the negative sign of ΔG^0_{ads} indicates the spontaneity of the adsorption process and stability of the adsorbed film on the electrode surface [67]. Furthermore, values of ΔG^0_{ads} upto -20 kJ mol^{-1} are reliable with the electrostatic interaction between the charged molecules and the charged metal (physisorption) while those more negative than -40 $kJmol^{-1}$ involve sharing or transfer of electrons from the inhibitor molecules to the metal surface to forma co-ordinate type of bond (chemisorption) [68]. Accordingly, the value of $-\Delta G^0_{ads}$ = -38.31 kJ/mol we propose chemisorption of NPEPB molecules on the C38 steel surface. Infact, because of strong adsorption of H_2O molecules on the surface of C-steel, it maybe assumed that removal of water

molecules from the surface is accompanied by chemical interaction between the metal surface and the formed film [66]. Results obtained from gravimetric measurements show that the steel corrosion rate values decrease when the concentration of NPEPB increases (Fig.7). The corrosion inhibition can be attributed to the adsorption of the NPEPB at the steel/acid solution interface. The highest inhibition efficiency 87 % was obtained at 10^{-3}M of NPEPB. The inhibition efficiencies, calculated from weight loss measurements, show the same trend as those obtained from electrochemical studies (Fig.7).

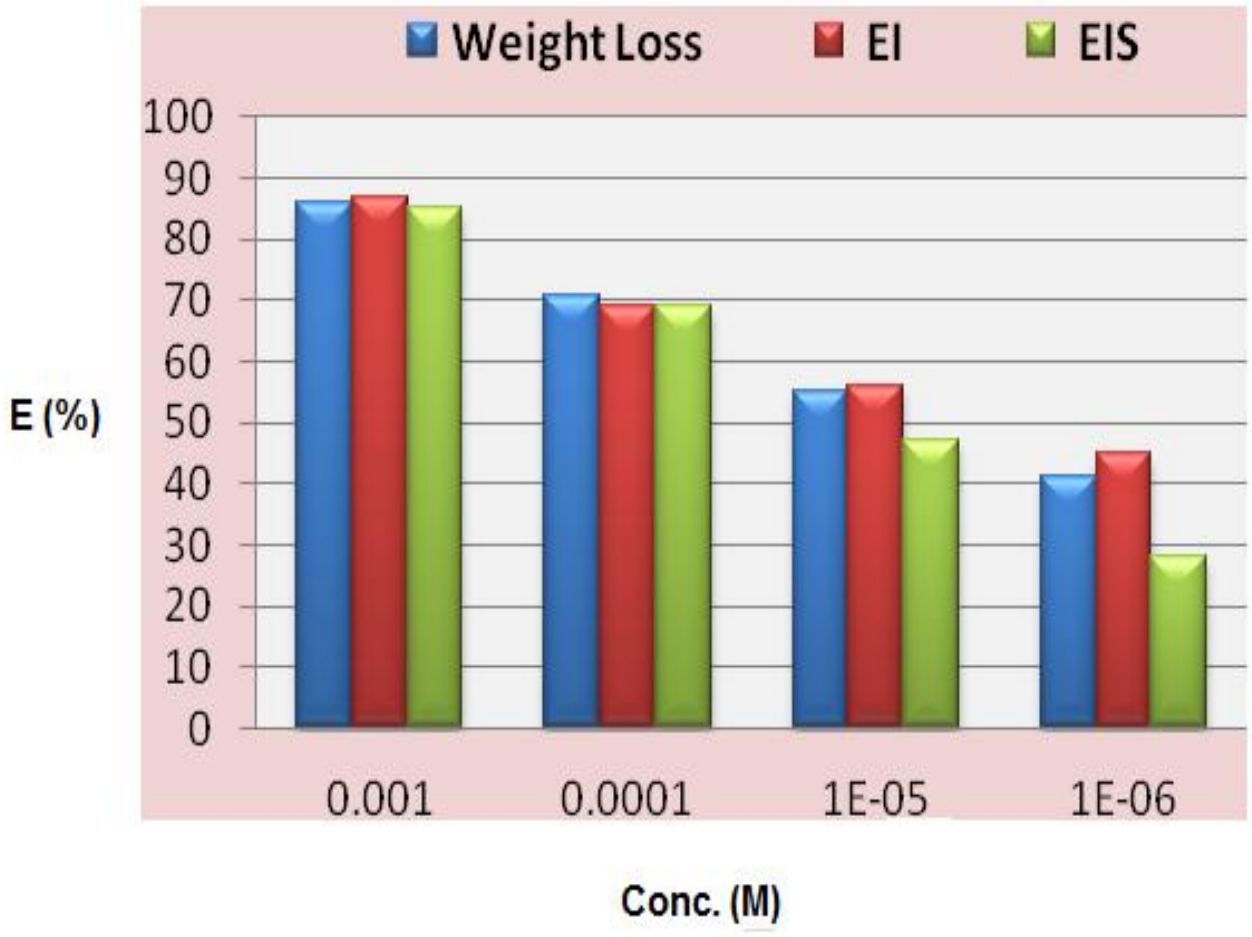

Figure 7. Comparison of inhibition efficiency (E %) values obtained by weight loss, EI and EIS methods.

3.4. Effect of temperature

To investigate the nature of adsorption of the inhibitor and to calculate the activation energies of the corrosion process, EIS measurements were obtained at different temperatures in the absence and the presence of NPEPB and precisely in the range of temperature 298-328 K. Figs 8 and 9 give the Nyquist plots for C38 steel in the absence and presence of 10-3M of NPEPB at different temperatures. The corresponding data are given in Table 5.

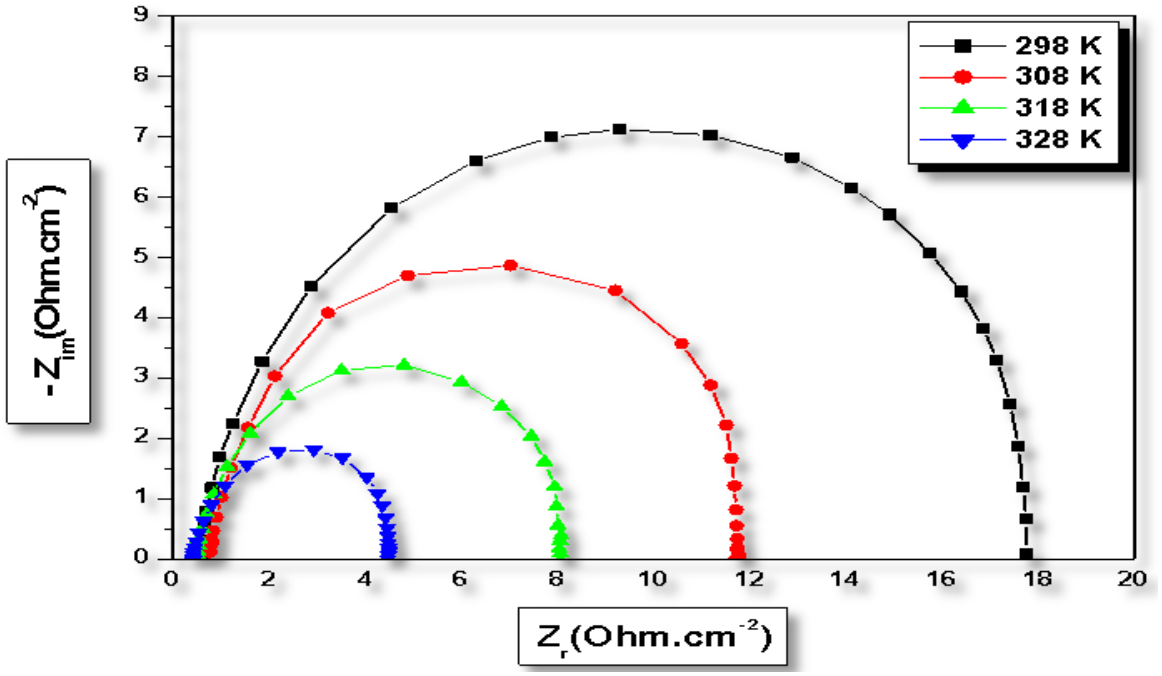

Figure 8. Nyquist diagrams for C38 steel in 1.0 M HCl at different temperatures.

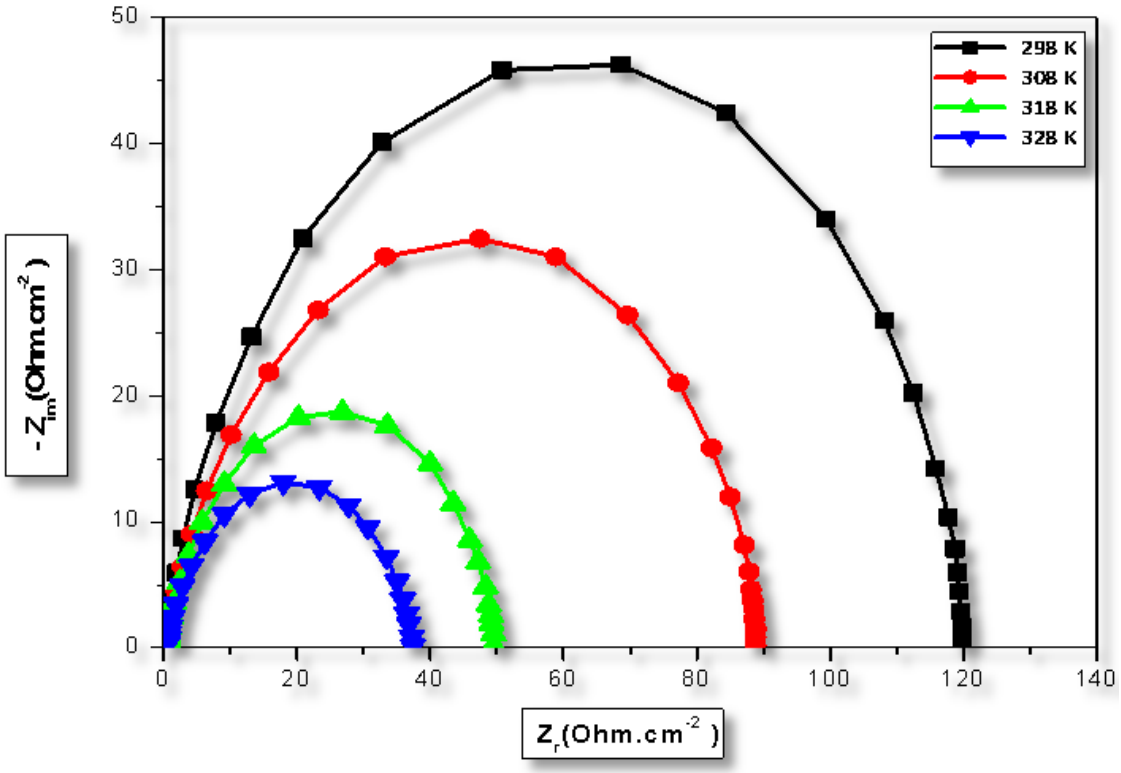

Figure 9. Nyquist diagrams for C38 steel in 1 M HCl + 10^{-3} M of NPEPB at different temperatures.

Temperature is a factor that plays a significant role in the corrosion of a given material in a corrosive environment. The behavior of the former might be affected by temperature in addition to

the possible modification in the metal-inhibitor interaction. It should be noted, however, that the temperature effect on the acid-metal inhibition reaction might be quite complex owing to the various changes occurring on the metal surfaces. For instance, rapid etching, inhibitor desorption and possible inhibitor decomposition [69,70].

Table 5. Thermodynamic parameters for the adsorption of NPEPB in 1.0 M HCl on the C38 steel at different temperatures.

Inhibitor	Temp (K)	R_{ct} ($\Omega.cm^2$)	C_{dl} ($\mu F/cm^2$)	E_{Rct} (%)
Blank	298	18	177	-
	308	12	190	-
	318	8	199	-
	328	4.5	223	-
NPEPB	298	120	530	85
	308	90	442	87
	318	50	503	84
	328	37.5	670	88

A very interesting feature depicted in table 5 is the increase of the inhibition efficiency with increasing temperature as expected, which is of practical interest in processes requiring the protection of the material at high temperature[71]. A maximum value of the effecacity 88 % was reached in the present study at 328 K as displayed in Fig. 10. Similar increase in the inhibition efficiency has been observed in literature at several metals, like copper [72], aluminum [71] and steel [69,73-75]. The most probable interpretation of this behavior is that the inhibition mechanism proceeds through a chemical adsorption (chemisorption) of NPEPB molecules onto the carbon steel surface and this indeed increases with rising temperature [69], this are confirmed whith the calculated of The ΔG^0_{ads} values.

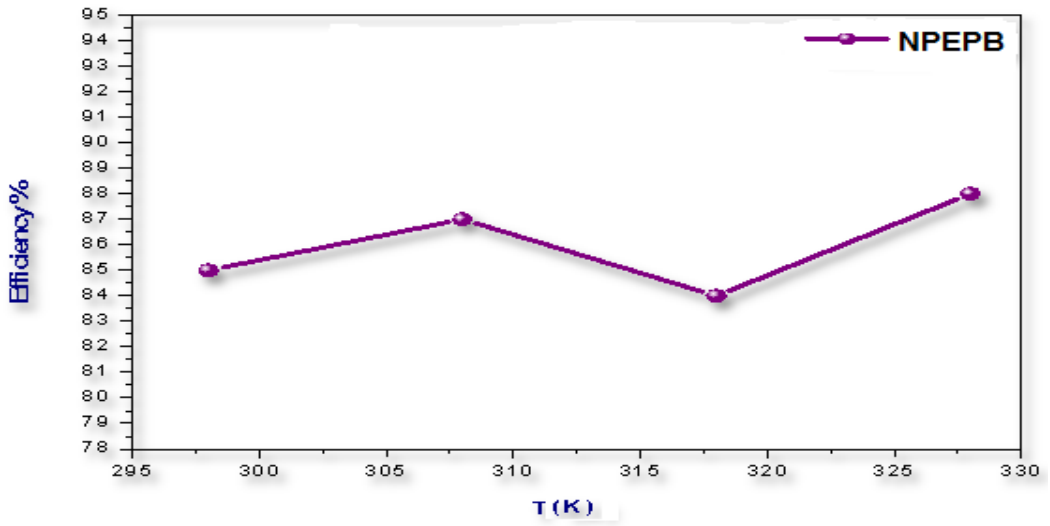

Figure 10. Effect of temperature (298- 328 °K) on the inhibition efficiency (EI%) of carbon steel corrosion in a (10^{-3} M of NPEPB + 1 M HCl) solution.

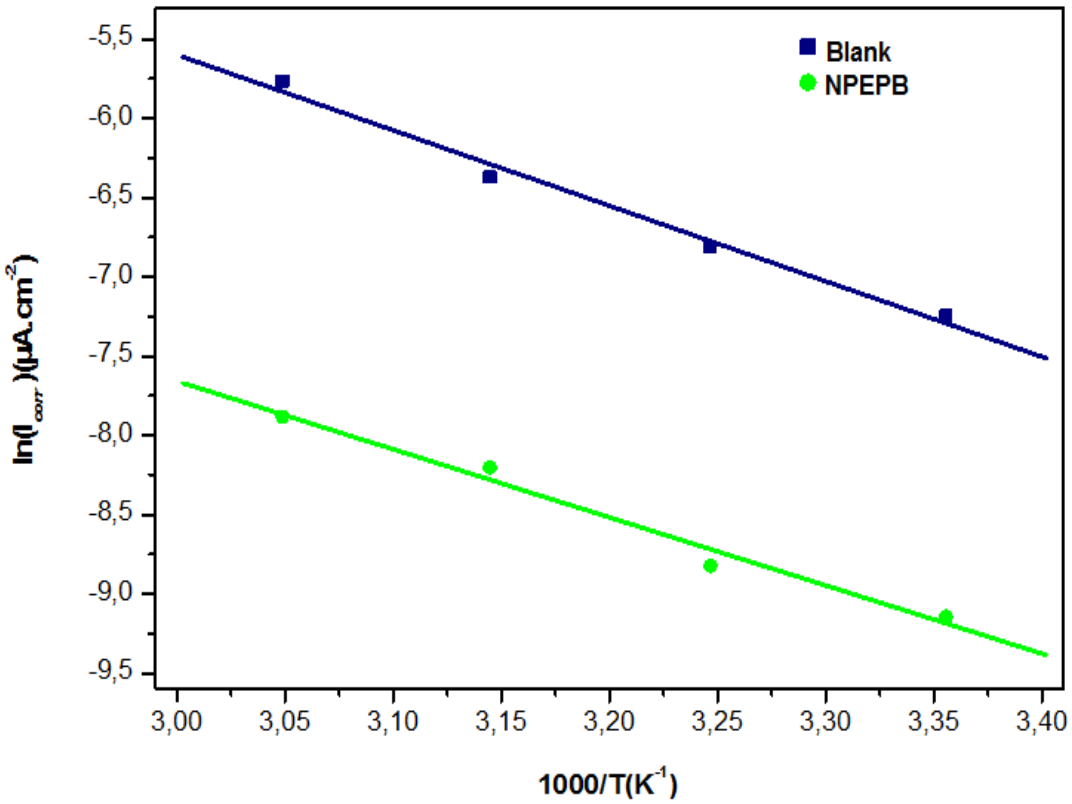

Figure 11. Arrhenius plots of C38 steel in 1M HCl with and without 10^{-3}M of NPEPB.

Also inhibition efficiency of NPEPB increased with increase in temperature. Values of R_{ct} were employed to calculate values of the corrosion current density (I_{corr}) at various temperatures in absence and presence of NPEPB using the following equation [68]:

$$I_{corr} = R_{ct}.T(z.F.R_{ct})^{-1} \quad (9)$$

Where R is the universal gas constant (R = 8.31 J K-1mol^{-1}), T is the absolute temperature, z is the valence of iron (z = 2), F is the Faraday constant (F = 96.485 coulomb) and R_{ct} is the charge transfer resistance.

Fig. 11 also shows that the corrosion reaction can be regarded as an Arrhenius-type process (Eq 9). The activation parameters for the studied system (E_a, ΔH_a^* and ΔS_a^*) were estimated from the Arrhenius equation and transition state equation (Eq 10-11) :

$$I_{corr} = A\exp(-\frac{E_a}{RT}) \quad (10)$$

$$I_{corr} = \frac{RT}{Nh}\exp\left(\frac{\Delta S_a^*}{R}\right)\exp\left(-\frac{\Delta H_a^*}{RT}\right) \quad (11)$$

Where A is Arrhenius factor, E_a is the apparent activation corrosion energy, N is the Avogadro's number, h is the Plank's constant, and ΔH_a^* and ΔS_a^* are the enthalpy and the entropy changes of activation corrosion energies for the transition state complex. R is the perfect gas constant.

The apparent activation energy was determined from the slopes of Ln I_{corr} vs 1/T graph depicted in Fig. 11.

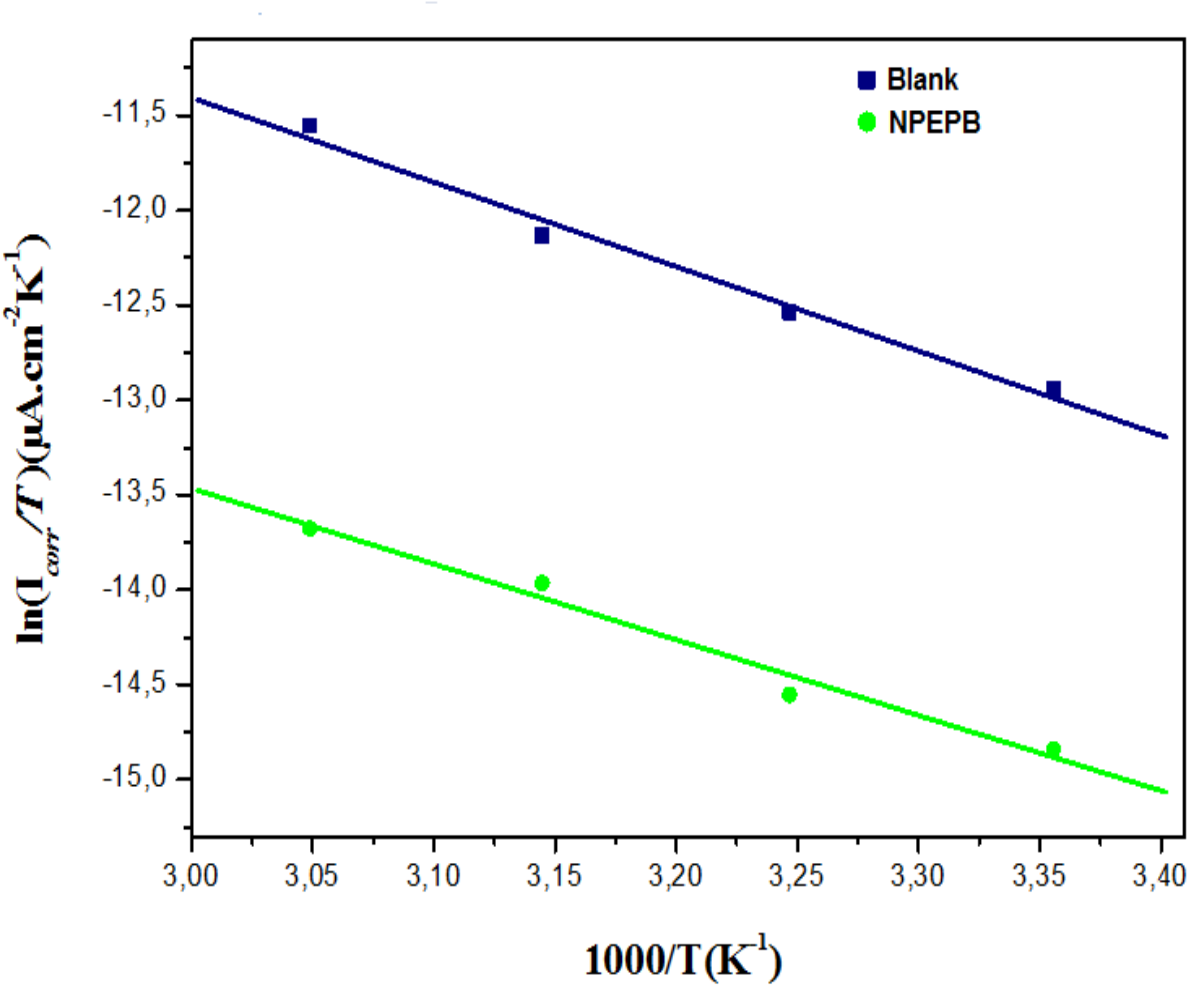

Figure 12. Relation between Ln (I_{corr}/T) and 1000/T at different temperatures.

A plot of ln (I_{corr}/T) against 1/T (Fig. 12) gave a straight line with slope (ΔH_a^* /R) and intercept (ln(R/N A h) + (ΔS_a^* /R)), from which the values of ΔH_a^* and ΔS_a^* were calculated and listed in Table 6.

Table 6. Activation parameters for the corrosion of C-steel in 1.0 M chloridric acid containing different concentrations of inhibitor NPEPB.

Inhibitor	E_a	ΔH^*_a	ΔS^*_a	$E_a - \Delta H^*_a$	ΔG
	(kJ/mol)	(kJ/mol)	(J/mol)	*(KJ/mol)*	*(kJ/mol) (T=298K)*
Blank	39.56	36.96	-181.35	2.60	91.01
NPEPB	35.69	33.09	-210.07	2.60	95.69

The decrease observed in the apparent activation energy E_a in the presence of inhibitor is a prove that the inhibitory effect of the investigated NPEPB for carbon steel corrosion in 1 M HCl proceeds indeed via a chemisorption [69,74]. As we reported, the value of the free energy ΔG^0_{ads} was more negative than -40 $kJmol^{-1}$; the inhibition efficiency increase with increasing temperature and the apparent activation energy E_a decrease with addition of inhibitor, from that; the adsorption mechanism of inhibition that we investigate in this studie are chemisorption. The positive sign of the enthalpie ΔHa reflect the endothermic nature of the steel dissolution process and mean that the dissolution of steel is difficult [76]. Another observation is that, for both blank and NPEPB containing solution, the values of ΔH_a^* are lower than the values of the respective activation energie which correspond to a decrease in the total reaction volume due to a gaseous process which is nothing but the hydrogen evolution reaction [77]. The difference of the two values is almost constant with an average value of 2.60 $kJ.mol^{-1}$ which is very close to the average value of the product(RT) in the investigated temperature range. Such behavior is characteristic of a unimolecular gas-phase reaction obeying the following equation: [69]

$$E_a - \Delta H_a^* = RT \qquad (12)$$

The negative value of entropie ΔS_a in the presence of inhibitor imply that the activated complex in the rate determining step represents an association rather than a dissociation step, meaning that an increase in disordering takes place on going from reactants to the activated complex [78].

3.5. Optical microscopy measurements

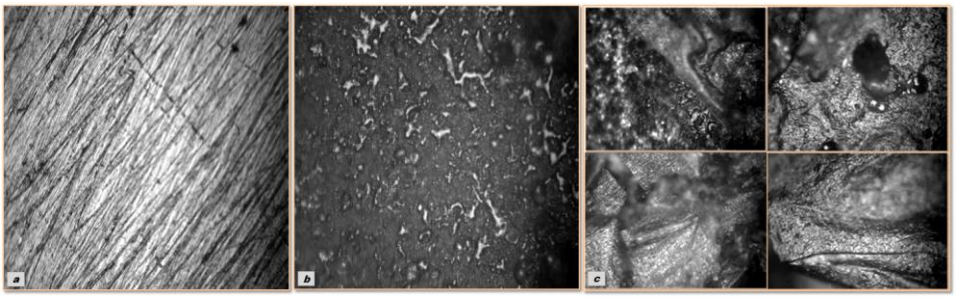

Figure 13. OM (x200) of tinplate (a) before immersion (b) after 6 hours of immersion in 1M HCl (C) after 6 hours of immersion in 1M HCl + 10^{-3} M of NPEPB at 298 K.

The surface morphology of C38 steel was showed by optical microscopy after 6 hours immersion in 1.0 M HCl before and after addition of the inhibitor. Fig. 13(a) give the micrograph obtained of polished steel without being exposed to the corrosive solution, while Fig. 13(b) illustrates a strongly damaged steel surface due to the formation of corrosion products after immersion in 1.0 M HCl solution. OM images of steel surface after immersion in 1.0 M HCl with 10^{-3} M of NPEPB is shown in Fig. 13(c). It can be seen from Fig.13a that the C-steel sample before immersion seems smooth and shows some abrading scratches on the surface. An aggressive attack of the corroding medium on the steel surface was shown in Figure11b after immersion in uninhibited 1.0M HCl. In

contrast, in the presence of 10^{-3} M of NPEPB (Fig. 13c), the steel surface was corroded only insignificantly. On top of that, an adsorbed layer on the steel surface was created that was not observed in Fig.13b. The result was a strengthening of surface coverage on the steel surface such that reduce a contact between the steel and the aggressive medium. Consequently, a good protective film was formed can efficiently inhibit the corrosion of steel.

4. CONCLUSION

From the general experimental results the following conclusions can be deduced:

The 1-(2-(4-nitrophenyl)-2-oxoethyl)pyridazinium bromide (NPEPB) are found to be a good inhibitor for the corrosion of Ccarbon steel in 1.0 M HCl and the inhibition efficiency increases with increasing of the NPEPB concentration. The E(%) determined by Tafel polarisation, EIS methods and weight loss are in good agreement.

The polarization curves study show that NPEPB compound can be classified as mixed inhibitor. The calculated electrochemical parameters show that the addition of inhibitor NPEPB reduces the capacitance Cdl values and increase the R_{ct}. It is suggested to attribute this to the increase of the thickness of the adsorption film at steel surface.

The inhibition of the corrosion prosses is accomplished by the adsorption of NPEPB molecules on the c-steel on the electrod surface, and the adsorption obeys to the Langmuir isotherm. The negative value of the $\Delta G°_{ads}$ indicates that the adsorption of the NPEPB molecules is spontaneous, endothermic process accompanied by a decrease in entropy. The thermodynamic results get from this study confirm the chemisorptive nature of the NPEPB adsorption on the Carbon steel.

Surface morphological studie with optical microscopy images showed that a film of inhibitor is formed on the electrode surface

References

1. M. Batros and N. Hakerman, *J. Electrochem. Soc*. 139 (1992) 3429.
2. F. Bentiss, M. Lagrenee, M. Traisnel, B. Mernari, H. El Attari. *J. Appl. Electrochem.* 29 (1999) 1073.
3. P. Kutej, J. Vosta, J. Pancir, J. Macak, and N. Hackerman, *J. Electrochem. Soc.* 142 (1995) 829.
4. M. Dahmani, A. Et-Touhami, S.S. Al-Deyab, B. Hammouti, A. Bouyanzer, *Int J. Electrochem. Sci*. 5 (2010) 1060.
5. J.M. Bastidas, J.L. Polo and E. Cano, *J. Electrochem. Soc.* 30 (2000) 1173.
6. M. A. Amin, S.S. Abd El Rehim, H.T.M. Abdel-Fatah, *Corros. Sci*. 51 (2009) 882.
7. M. Ozcan, F. Karadag, I. Dehri, *Colloid Surface A.* 316 (2008) 55.
8. E. E. Oguzie, Y. Li, F.H. Wang, *Electrochim. Acta*. 53 (2007) 909.
9. E. E. Oguzie, Y. Li, F.H. Wang, *J. Colloid & Interf. Sci.* 310 (2007) 90.
10. A. B. Silva, S.M.L. Agostinho, O.E. Barcia, G.G.O. Cordeiro, E. D'Elia, *Corros. Sci*. 48 (2006) 3668.
11. O. Olivares, N.V. Likhanova, B. Gomez, J. Navarrete, M.E. Llanos-Serrano, E Arce., J.M. Hallen, *Appl. Surf. Sci*. 252 (2006) 2894.
12. S. Aezola, J. Genesca, *J. Solid State Electrochem.* 8 (2005) 197.
13. H. Zarrok, H. Oudda, A. Zarrouk, R. Salghi, B. Hammouti, M. Bouachrine, *Der Pharma Chemica*. 3 (2011) 576.

14. M. Zerfaoui, B. Hammouti, H. Oudda, M. Benkaddour, *Prop. Org. Coat*. 51 (2004) 135.
15. K. Bouhrira, F. Ouahiba, D. Zerouali, B. Hammouti, M. Zertoubi, N. Benchat, *J .Chemistry*. 7 (2010) S35.
16. S. A. Abd El Maksoud, *J. Electroanal. Chem*. 565 (2004) 321.
17. Y. Abboud, B. Ihssane, B. Hammouti, A. Abourriche, S. Maoufoud, T. Saffaj, M. Berrada, M. Charrouf, A. Bennamara, H. Hannache, *Desal & Water Treat*. 20 (2010) 35. 1202.
18. M. Zerfaoui, H. Oudda, B. Hammouti, M. Benkaddour, S. kertit, M. Zertoubi, M. Azzi, M. Taleb, *Revue de Metall*. 99 (2002) 1105.
19. A. Yahyi, A. Aouniti, B. Hammouti, A. Ramdani, S. Kertit, *Trans. SAEST.* 39 (2004) 5.
20. A. Anejjar, R. Salghi, A. Zarrouk, O. Benali, H. Zarrok, B. Hammouti, E. E. Ebenso, *J. Assoc. Arab. Univer Bas & Appl Sci.* 15(2014)21.
21. R. Salghi, B. Hammouti, A. Aouniti, M. Berrabah, S. Kertit, *J. Electrochem. Soc. India*. 49 (2000) 40.
22. B. Zerga, A. Attayibat, M. Sfaira, M. Taleb, B. Hammouti, M. Ebn Touhami, S. Radi, Z. Rais, *J. Appl. Electrochem*. 40 (2010) 1575.
23. K. Tebbji, A. Aouniti, A. Attayibat, B. Hammouti, H. Oudda, M. Benkaddour, S. Radi, A. Nahle, *Ind J. Chem. Techn*. 18 (2011) 244.
24. L. Herrag, B. Hammouti, S. Elkadiri, A. Aouniti, C. Jama, H. Vezin, F. Bentiss, *Corros. Sci*. 52 (2010) 3042.
25. M. Benabdellah, A. Yahyi, A. Dafali, A. Aouniti, B. Hammouti, A. Bnettouhami. *Arab. J. Chem*. 4 (2011) 343.
26. H. Ashassi-Sorkhabi, Z. Ghasemi, D. Seifzadeh, *Appl. Surf. Sci*. 249 (2005) 408.
27. M. Bouklah, A. Attayibat, B. Hammouti, A. Ramdani, S. Radi, M. Benkaddour, *Appl. Surf. Sci*. 240 (2005) 341.
28. A. El-Ouafi, B. Hammouti, H. Oudda, S. Kertit, R. Touzani, A. Ramdani, *Anti-Corros. Met.Mater*. 49 (2002) 199.
29. N. Huynh, S.E. Bottle, T. Notoya, A. Trueman, B. Hinton, D.P. Schweinsberg, *Corros. Sci*. 44 (2002) 1257.
30. R. Salghi, L. Bazzi, B. Hammouti, E. Zine, S. Kertit, S. El Issami, E. Ait Eddi, *Bull. Electrochem.* 17 (2001) 429.
31. A. Chetouani, K. Medjahed, K.E. Sid-Lakhdar, B. Hammouti, M. Benkaddour, A. Mansri, *Corros.Sci*. 46 (2004) 2421.
32. A. Ousslim, A. Aouniti, K. Bekkouch, A. Elidrissi, B. Hammouti, *S. Review & Letters*. 16 (2009) 609.
33. K.Tebbji, H. Oudda, B. Hammouti, M. Benkaddour and S. S. Al-Deyab, A. Aouniti, S. Radi, A.Ramdani, *R. Chem. Intermed*. 37 (2011) 985.
34. M. Elayyachy, B. Hammouti, A. El Idrissi, A. Aouniti, *Port. Electrochim. Acta*. 29 (2011) 57.
35. M.T. Saeed, *Anti-Corros. Met. Mater*. 51 (2004) 389.
36. L.G. Qiu, A.J. Xie, Y.H. Shen, *Corros. Sci*. 47 (2005) 273.
37. S. Muralidharan, M.A. Quaraishi, S.V.K. Iyer, *Corros. Sci*. 37 (1995) 1739.
38. I. Sekine, Y. Nakata, H. Tanabe, *Corros. Sci*. 28 (1988) 987.
39. T. Tsuda, C.L. Hussey, *Interface*. 16 (2007) 42.
40. S. Zhang, N. Sun, X. He, X. Lu, X. Zhang, *J. Phys. Chem. Ref. Data*. 35 (2006) 4.
41. H. Zhao, *Chem. Eng. Comm*. 193 (2006) 1660.
42. H. Ashassi-Sorkhabi, M. Es'haghi, *Mater. Chem. Phys*. 114 (2009) 267.
43. N.V. Likhanova, M.A. Dominguez-Aguilar, O. Olivares-Xometl, N. Nava-Entzana, E. Arce, H. Dorantes, *Corros. Sci.* 52 (2010) 2088.
44. Q.B. Zhang, Y. X. Hua, *Electrochim Acta*. 54 (2009) 1881.
45. R. Gasparac, C.R. Martin, E. Stupnisek-lisek, *J. Electrochem. Soc*. 147 (2000) 548.
46. M. E. Palomar, C.O. Olivares-Xometl, N.V. Likhanova, J.B. Perez-Navarrete, *J. Surfact.*

Deterg. 14 (2011) 211.
47. M .A. Quraishi, M.Z.A. Rafique, S. Khan, N. Saxena, *J. Appl Electrochem.* 37 (2007) 1153.
48. I. Olariu, M. Caprosu, G. Grosu, M. Ungureanu, M. Petrovanu, Roum. Biotech. Lett. 4 (1999) 365.
49. M. A.M. Ibrahim, M. Messali, Z. Moussa, A.Y. Alzahrani, S.N. Alamry, B. Hammouti, *Portug. Electrochim. Acta.* 29 (2011) 375.
50. M. Messali, *Arab. J. Chem*., **7** (1) (2014) 63.
51. A. Zarrouk, M. Messali, M.R. Aouad, M. Assouag, H. Zarrok, R. Salghi, B. Hammouti, A. Chetouani, *J. Chem. Pharm. Res*. 4 (2012) 3427.
52. M. Messali, M. R. Aouad, A. A. Ali, N. Rezki, T. Ben Hadda; B. Hammouti, *Medicinal Chemistry Research*, 24 (4) (2015) 1387.
53. A.F. Al-Ghamdi, M. Messali, S.A. Ahmed, *J. Mater. Environ. Sci*. 2 (2011) 215.
54. F. Bentiss, F. Gassama, D. Barbry, L.Gengembre, H.Vezin, M. Lagrenee, M. Traisnel, *Appl. Surf. Sci.* 252 (2006) 2684.
55. 55 G.and J.Zhou,.N.Mu,X.H.Li,Q.Qu, *Corros.Sci*. 48(2006) 445
56. S. A. Umoren, I. B. Obot, E.E.Ebenso, P. C. Okafor, O. Ogbobe, E. E. Oguzi, *Anti.corros. Meth. Mater.* 53 (2006) 277.
57. J.O.M Bockris, D. Drazic, *Electrochem. Acta.* 7(1962) 293
58. T. suru, T.Haruyama, S.Gijutsu, *B.J. Jpn. Soc. Corros. Eng*. 27 (1978) 573.
59. J. Aljourani, K. Raeissi, M.A. Golozar, *Corros. Sci*. 51 (2009)1836.
60. A. Anejjar, A. Zarrouk , R. Salghi , D. Ben Hmamou, H. Zarrok, S. S. Al-Deyab, M. Bouachrine, B. Hammouti, N. Benchat, *Int. J. Electrochem. Sci*. 8 (2013) 5961.
61. E. McCafferty, N .*Hackerman J Electrochem Soc*. (1972) 119.
62. A. A .El-Awady, Abd-El-Nabey B A., Aziz S G. *J. Electrochem. Soc.* 139 (1992) 2149.
63. J.O'M. Bockris, A.K.N. Reddy, Modern Electrochemistry, Plenum Publishing Corporation, NewYork. 2 (1976).
64. X. Wang, H.Yang, F. Wang, *Corros. Sci*. 52 (2010) 1268.
65. B. S. Sanat kumar, J. Nayak, A.N. Shetty, *J. Coat. Technol. Res*. 4 (2011) 1.
66. A. AliAnejjar, R. Salghi, A. Zarrouk, H. Zarrok, O. Benali, B. Hammouti, S.S.Al-Deyab, N-E. Benchat, R. Saddik., , DOI10.1007/s11164-013-1244-7, *Res Chem Intermed*. 41 (2015) 913.
67. M. H. Hussin, M. Kassim, *J. Mater. Chem. Phys*. 125 (2011) 461.
68. O. Benali, L .Larabi, M .Traisnel, L .Gengenbre, Y. Harek, *Surf. Sci*. 253 (2007) 6130.
69. E. A. Noor, *Int. J. ELectrochem. Sci.* 2 (2007) 996-1017.
70. F. Z. Bouanis, F.Bentiss, M.Traisnel, C. Jama, *Electrochim. Acta.* 54 (2009) 2371.
71. G. K. Gomma, M.H. Wahdan, *Mater. Chem. Phys*. 39 (1995) 209.
72. M. M. Antonijevic, M.B. Petrovic, *Intern. J. ELectrochem. Sci*. 3 (2008) 1.
73. X. Li, G. Mu, *Appl. Surf. Sci*. 252 (2005) 1254.
74. L. Larabi, O. Benali, Y. Harek, *Mater. Lett* . 61 (2007) 3287.
75. D. Ben Hmamou, M.R. Aouad, R. Salghi, A. Zarrouk, M. Assouag, O. Benali, M. Messali, H. Zarrok, B. Hammouti, *J. Chem. Pharm. Res*. 4 (2012) 3489.
76. N.M. Guan, L. Xueming, L. Fei, *Mater. Chem. Phys.* 86 (2004) 59.
77. S. Ben Aou, *Int. J. Electrochem. Sci*. 8 (2013) 10788 - 10804
78. A. Anejjar , R. Salghi, S. Jodeh, S. S. Al-Deyab, B. Hammouti, A. M. Elhassan, *Mor. J. Chem*. 2 (3) (2014) 236-251.